

Hypoxic preconditioned hUC-MSCs enhance its therapeutic efficacy in Lipopolysaccharide induced ALI via the TLR4/MyD88 and phosphorylation of PI3K/Akt mediated by TREM-1

Yujuan Wang (✉ yujuan19@mails.jlu.edu.cn)

Jilin University Second Hospital <https://orcid.org/0000-0002-6730-1209>

Rong Gao

Jilin University Second Hospital

Bingdi Yan

Jilin University Second Hospital

Han Li

Jilin University Second Hospital

Junling Yang

Jilin University Second Hospital <https://orcid.org/0000-0001-8360-2901>

Research Article

Keywords:

Posted Date: June 14th, 2022

DOI: <https://doi.org/10.21203/rs.3.rs-1639913/v1>

License:   This work is licensed under a Creative Commons Attribution 4.0 International License.

[Read Full License](#)

Abstract

Background

Acute lung injury/acute respiratory distress syndrome (ALI/ARDS) is caused by a variety of direct or indirect factors, such as infection including Corona Virus Disease 2019 (COVID19), trauma, inhalation of harmful gases, and shock. Progression of COVID19 severity can lead to ALI/ARDS. Owing to its unclear pathogenesis, there is currently no effective treatment established for this disease. As per a past report, human umbilical cord mesenchymal stem cells (hUC-MSCs) can decrease the extent of the injury of ALI in the mice. Hypoxic preconditioning umbilical cord MSCs (HP-hUC-MSCs) demonstrated significantly enhanced proliferation and differentiation capabilities. Furthermore, the expression of several growth factors was significantly upregulated, which remarkably increased the repair of damaged lung tissues.

Methods

The hUC-MSCs were cultured by cell adhesion. The properties of hUC-MSCs were identified by morphology, flow cytometry, osteogenesis, and adipogenic differentiation. We employed a transwell chamber to establish a co-culture system of hUC-MSCs and BEAS-2B. Accordingly, we evaluated the hUC-MSCs ability to treat ALI/ARDS in a lipopolysaccharide (LPS)-induced mouse model. The measurements of lung histopathological changes and neutrophil infiltration, wet/dry(W/D), pro-inflammatory, and anti-inflammatory cytokines in the bronchoalveolar lavage fluid (BALF) were performed.

Results

The cultured hUC-MSCs demonstrated excellent osteogenic and adipogenic differentiation abilities. When compared with normal hUC-MSCs, HP-hUC-MSCs can further reduce the inflammatory response of BEAS-2B and ALI model mice induced by LPS and enhance their anti-apoptotic ability. The level of soluble triggering receptor expressed on myeloid cells (sTREM-1) in patients with severe pneumonia increased, indicating a positive correlation with the disease severity.

Conclusions

Our positive preclinical results suggest that HP-hUC-MSCs can exert a stronger therapeutic effect on ALI by reducing the expression of TREM-1 and that the mechanism behind this phenomenon may be related to the TLR4/MyD88 and the phosphorylation of PI3K/Akt.

Background

Acute lung injury/acute respiratory distress syndrome (ALI/ARDS) can affect people of various ages, with an incidence rate of 18–38%. This condition is mostly manifested as difficult-to-cure hypoxemia [1]. Presently, the pathophysiology of ALI/ARDS is yet unknown and the related mortality rate remains as high as 40–60% [2]. The essence of ALI/ARDS is diffuse alveolar-capillary membrane damage, which is mostly characterized by respiratory insufficiency and a number of infiltrating inflammatory cells in the lung tissues [3]. The conventional treatment of ALI mainly includes mechanical ventilation therapy, vasodilators, surfactants, antioxidants, glucocorticoids (GC), and anti-inflammatory drugs. The human umbilical cord mesenchymal stem cells (hUC-MSCs) express a variety of unique markers of embryonic stem cells that possess the characteristics of differentiation, proliferation ability, low immunogenicity, convenient material collection, and no restrictions on ethical issues. MSCs have been proven in preclinical studies of respiratory illness to have therapeutic benefits via direct differentiation and paracrine effect [4]. These characteristics indicate that hUC-MSCs, as a new therapeutic method, present good clinical application prospects for the current treatment of irreparable cell and tissue damage and diseases such as ALI/ARDS and even pulmonary fibrosis. These hUC-MSCs entrapped in the lungs can release a range of soluble substances that effectively reduce lung damage [5]. In comparison to antifibrotic medications like nintedanib or pirfenidone, MSCs might effectively cure pulmonary fibrosis, with much better results in lung volume, pathological alterations, lung function, and blood oxygen saturation [6]. However, direct injection affects hUC-MSCs homing in the lung tissues and their stay in the damaged tissues, which lowers the therapeutic efficacy. Recent studies have reported that hypoxic preconditioning umbilical cord hUC-MSCs (HP-hUC-MSCs) show significantly enhanced proliferation and differentiation capabilities, reduced production of oxygen-free radicals in the cells, which significantly increased the repair of damaged tissues. In our research, we deeply explored the effect of hUC-MSCs on the treatment of ALI/ARDS so as to further reveal the molecular mechanism behind this effect and provide a theoretical basis and propose a new direction for ALI/ARDS therapy in the future.

Methods

Cell Culture

hUC-MSCs were cultured from human donor umbilical cord aspirates. The cells used in our experiment were donated by the Sigma Company (China, Changchun). The cultures were maintained at a standard condition with 37°C and 5% CO₂. hUC-MSCs were required to adhere for 24–48 h by the next passage, after which the non-adherent fraction was removed by washing with PBS twice. These cells were subsequently trypsinized with 0.25% trypsin. The cultures were maintained at approximately 80% confluence. After attaining 100% confluence, the cells were passaged again. All experiments were performed with 3–6 cell passages.

Flow cytometry (FC)

The cells released by cell dissociation buffer (0.1% BSA, diluted with 1× PBS) were phenotyped by flow cytometry (Beckman Coulter) and monoclonal antibodies as recommended by the manufacturers.

Antibodies for CD29, CD105, CD73, CD166, CD44, CD45, CD14, CD11b, CD34, and HLA-DR were purchased from Cyagen. HLA-DR and CD44 were labeled by two antibodies, PE and FITC, and the others were labeled by a single antibody, PE.

Osteogenesis and adipogenesis

The osteogenic stem cell kit was purchased from Cyagen. After cultured 2–4 weeks, hUC-MSCs were stained by Alizarin red and assessed for bone nodule formation. The adipogenesis stem cell kit was purchased from Cyagen as well. The medium A was changed every 3 days, while the medium B was changed every 24 h. The cultures were observed for fat cell formation. After alternating 3–5 times with media A and B, the culture was continued with medium B for 4–7 days. Then, hUC-MSCs were subjected to Oil red staining.

Hypoxia

Two hypoxic preconditioning methods were employed in our study: a hypoxia incubator and CoCl_2 , which was added to make the final concentration to 100 $\mu\text{mol/L}$.

Co-culture of hUC-MSCs or HP-hUC-MSCs and BEAS-2B Cells

To determine the effect of hUC-MSCs and HP-hUC-MSCs on BEAS-2B, we selected a 6-well transwell to co-culture hUC-MSCs and BEAS-2B. BEAS-2B was cultured in the lower layer of the transwell and hUC-MSCs in the upper. The experimental were categorized into control, lipopolysaccharide (LPS), LPS + hUC-MSCs, and LPS + HP-hUC-MSCs groups. After allowing 24 h for adherence, we added 2 μL of LPS (1 $\mu\text{g/mL}$) to the LPS, LPS + hUC-MSCs, and LPS + HP-hUC-MSCs groups, and placed the transwell containing hUC-MSCs and HP-hUC-MSCs into the LPS + hUC-MSCs group and LPS + HP-hUC-MSCs group, respectively. After 48 h, we assessed the viability of BEAS-2B with the Cell Counting Kit-8 (CCK8) assay and apoptosis by Western blotting.

Assay for proliferation

We used the CCK8 as per the manufacturer's protocol to assay the cell proliferation of hUC-MSCs. Briefly, the passage 6 hUC-MSCs were seeded in a 6-well plate. At the endpoint, 200 μL of CCK-8 was added to each well for a further 1 h. The final result was presented as OD450 by microplate reader (Thermo).

Enzyme-linked immunosorbent assay (ELISA)

The supernatant from cell culture to be tested was centrifuged at 1,000 $\times g$ for 20 min at 4°C to remove the insoluble debris. The supernatants were analyzed using the human VEGF, HGF, NGF, and KGF enzyme-linked immunosorbent assay kits.

ALI mice model caused by LPS

Male 6–8-week-old BALB/C mice were anesthetized with 5% chloral hydrate (bought from Changchun Yisi Laboratory Animal Corporation, Changchun, China). The experimental mice were assigned to 5

groups, with 4 mice in each group: A. Control group; B. ALI model group; C. hUC-MSCs group; D. CoCl₂ preconditioned hUC-MSCs group; E. Hypoxic incubator preconditioned hUC-MSCs group. LPS from *Escherichia coli* O55:B5 (Sigma) was used to create ALI at a dose of 5 mg/kg delivered intratracheally. PBS, hUC-MSCs, CoCl₂ preconditioned hUC-MSCs, and hypoxic incubator preconditioned hUC-MSCs (C, D, and E groups) (1×10^6 cells, 200 μ L total volume) were progressively injected into the mice via the tail vein 4 h later, with normal mice serving as control. The mice's living conditions were observed and they were sacrificed 72 hours since began. Blood and BALF samples were gathered and processed at 2000 rpm for 3 min to obtain the supernatant samples. To calculate the wet weight, the right middle lobe was removed and weighed instantly. The lung tissues were then dried in a 60°C oven for 48 h for dry weight. The wet/dry is an indicator of pulmonary edema. The left lung was fixed for hematoxylin and eosin (HE) detection. Immunohistochemistry (IHC) was performed to detect the expression of TREM-1 in the lungs.

Detection of BALF protein and neutrophil number

We employed the BCA kit (Beyotime, China) to determine the protein content in the BALF, which reflected the permeability of the endothelial and epithelial cells. After BALF centrifugation, the cell pellets were resuspended and spread uniformly on glass slides, followed by Wright's staining. The number of neutrophils was then enumerated and counted under a microscope (thermo, the United States).

Detection of myeloperoxidase (MPO) activity

We employed the MPO kit (Nanjing Jiancheng, Nanjing, China) to assess the MPO vitality

according to the manufacturer's protocol, which was used to assess the extent of neutrophil infiltration of the lung.

IHC of triggering receptor expressed on myeloid cells (TREM-1)

The IHC of the lung tissues was deparaffinized by paraffin sectioning, followed by EDTA treatment for antigen retrieval. Then, 3% H₂O₂ was used to block endogenous peroxidase. After blocking with BSA for 2 h, the tissues were treated with the TREM-1 primary antibody and corresponding secondary antibody, subsequently observation under the microscope(thermo, the United States).

Real-Time PCR Analysis

The RNA extraction kit and reverse-transcriptase kit were used to obtain total RNA and cDNA. A real-time PCR detection system (Bio-Rad, USA) was applied to conduct real-time PCR. Table 1 lists the primers used in the research, with β -actin acting as a control. The cycling conditions were 95°C for 2 min, 40 cycles of 95°C for 15 s, and 60°C for 30 s. The reactions were carried out in triplicate, and the data was evaluated with the algorithm of $2^{-\Delta\Delta Ct}$.

Table 1
The Real-Time PCR primers (Species:Mouse)

genes	Forward	Reverse
TREM-1	CCTGTTGTGCTCTTCCATCCTGTC	GGACGCTCTGTCAGCCTTGTAATAG
MyD88	AGCAGAACCAGGAGTCCGAGAAG	GGGCAGTAGCAGATAAAGGCATCG
TLR4	GAGCCGGAAGGTTATTGTGGTAGTG	AGGACAATGAAGATGATGCCAGAGC
Bcl-2	CTGTGCCACCATGTGTCCATCTG	TCTCTGCGAAGTCACGACGGTAG
Akt	TCAGGATGTGGATCAGCGAGAGTC	AGGCAGCGGATGATAAAGGTGTTG
PI3K	CGAAACAAAGCGGAGAACCTATTGC	TCTACCACTACGGAGCAGGCATAG
caspase3	TCTGACTGGAAAGCCGAAACTCTTC	GTCCCACTGTCTGTCTCAATGCC

The primer sequences of experiment involved indicators, all of which were mouse origin. TREM-1 triggering receptor expressed on myeloid cells, MyD88 Myeloid differentiation factor, TLR4 Toll-like receptor 4

Western blotting

By centrifuging the same passage hUC-MSCs cell lysate at 12000 rpm continue 15 min at 4°C, total protein was finally extracted. Then, the protein density were measured using the BCA Protein Assay Kit (Beyotime,China). Equal amounts of proteins were loaded in 12% polyacrylamide gel, separated by electrophoresis, and then printed onto PVDF membranes. The redundant proteins in membranes were neutralized with 5% nonfat milk in TBST for at least 1 h at room temperature, and subsequently incubated at 4°C overnight with the following primary antibodies: PI3K, AKT, p-AKT, Bcl-2, and c-caspase3 purchased from Affinity and a goat anti-rabbit secondary antibody (1:1500 dilution). The blots were probed with the ECL assay kit as per the manufacturer's directions. The protein bands to be quantified using the Image J software.

Results

The characterization of hUC-MSCs

Healthy umbilical cord aspirates were used to isolate hUC-MSCs. The stem cells used in our experiment were donated by the Changchun Sigma Company and passaged by us. Under inverted microscopy, the morphology of hUC-MSCs was found to be spindle-shaped and fibroblast-like (Fig. 1a). If allowed to continue to grow, hUC-MSCs can present a whirlpool. To prevent senescent or differentiation of hUC-MSCs in the later passages, we used hUC-MSCs between passages 3 and 6 throughout our study. The characterization by flow cytometry confirmed the absence of CD45, CD34, CD14, CD11b, and HLA-DR⁻ in hUC-MSCs, while they expressed CD29, CD105, CD73, CD166, and CD44 (Fig. 1b). This marker profile was consistent with those reported previously [7-10]. The cultures were observed for fuchsia bone nodules

(Fig. 1c) and red lipid droplets formation (Fig. 1d). As evidenced by experimental results, hUC-MSCs could differentiate into the adipogenic and osteogenic lineages *in vitro*. In summary, the “hUC-MSCs” we obtained are consistent with most literature, indicating that the cells were hUC-MSCs with the ability to differentiate into multiple directions.

hUC-MSCs can improve the function of BEAS-2B and the enhancement effect of HP-hUC-MSCs

We established an in-direct contact co-culture system of BEAS-2B and hUC-MSCs or HP-hUC-MSCs to estimate the impact of hUC-MSCs on BEAS-2B. The Transwell chamber was suspended and used with 6-well plates. The upper layer was seeded with 1 mL (5×10^5 cells/well) of hUC-MSCs or HP-hUC-MSCs, and the lower layer was seeded with 2 mL (1×10^6 cells/well) of BEAS-2B, with the semipermeable membrane separated (Fig. 2a). BEAS-2B is a normal human bronchial epithelial cell that grows adherently and is epithelioid and polygonal (Fig. 2b).

In the LPS and co-culture groups, some BEAS-2B cells died in the periphery, while others were shrunken, with rough and granular material deposition, indicating that the BEAS-2B was damaged by LPS. We then used the CCK8 to detect the vitality of BEAS-2B. We found that exposure to LPS reduced the BEAS-2B vitality, which was reversed by hUC-MSCs (****, $p < 0.0001$), while HP-hUC-MSCs showed a stronger effect relative to the normal hUC-MSCs group (****, $p < 0.0001$) (Fig. 2c).

After LPS, sTREM-1 and TNF- α increased in the cell culture supernatant when compared with that in the control group, while IL-10 reduced. Different from the LPS treatment group, the extent of anti-inflammatory factor IL-10 in the co-culture group increased, while the inflammatory factors sTREM-1 and TNF- α decreased. Compared with the normal hUC-MSCs co-culture group, HP-hUC-MSCs increased IL-10 and decreased sTREM-1 and TNF- α to a relatively greater extent. These observations signify that co-culture with hUC-MSCs could reduce the BEAS-2B injury from LPS, while HP-hUC-MSCs had a greater impact on relieving the harm of BEAS-2B (Fig. 2d).

In comparison with the control group, the secretion of VEGF, NGF, KGF, and HGF in the LPS group was obviously different. When contrasted with the LPS group, the level of VEGF, NGF, KGF, and HGF in the normal hUC-MSCs co-culture group has obvious statistical difference. In accordance with the normal hUC-MSCs co-culture group, a visible difference was showed in the expression of VEGF, NGF, KGF, and HGF in the HP-hUC-MSCs co-culture group (Fig. 2e).

When compared with the control group, BEAS-2B showed a higher apoptosis in LPS group, which was manifested as an increased expression of apoptotic proteins PI3K, AKT, p-AKT, c-caspase3, and lowered level of Bcl-2, an anti-apoptotic protein. hUC-MSCs could alleviate apoptosis of BEAS-2B, which was manifested as a decreased expression of apoptotic proteins PI3K, AKT, p-AKT, and c-caspase3 and Bcl-2, an anti-apoptotic protein, expressed at a higher level. Furthermore, the reversal and repair of BEAS-2B

damage in the HP-hUC-MSCs experimental group were found to be stronger than that in the normal hUC-MSCs test group (Fig. 2f).

Establishment of an LPS-mediated ALI mouse model

LPS is generally applied to build ALI model. In the ALI model mice, the lung volume increased, with obvious edema and focal hemorrhage on the lung surface. Under the microscope, infiltration of a large number of inflammatory cells was noted; the pulmonary interstitium widened; the alveoli collapsed, and the alveolar cavity exuded. Pulmonary capillary congestion, hemorrhage, and other pathological changes mainly manifested as inflammatory cell infiltration and pulmonary interstitial edema (Fig. 3a-b). Furthermore, stimulated neutrophils were discovered to have a critical role in initiating the proinflammatory processes that lead to hemorrhage or alveolar injury ^[11].

Other than in the lungs, no inflammatory cell infiltration was noted in the heart, liver, spleen, and kidney in the ALI model by LPS. The results showed that the inflammatory lesion is limited to the lungs (Fig. 3c). Therefore, our results prove that the intratracheal construction of this ALI model by LPS was feasible.

hUC-MSCs could improve ALI mice and the enhancement effect of HP-hUC-MSCs

We first weighed the dry and wet (not shown in the figure) weight of the lungs. Then, the W/D value was calculated to evaluate the extent of lung edema in each mice group. We also examined the MPO of the lung tissues to assess the degree of inflammatory cell infiltration and migration. Our results suggest that the W/D and MPO increased significantly after LPS stimulation. After the administration of normal hUC-MSCs, the W/D and MPO of the lung evidently decreased, showing a statistical difference. These factors decreased further, showing a statistically significant difference after the administration of HP-hUC-MSCs (Fig. 4a-b).

BALF is an important marker for evaluating lung functions, while the number of neutrophils in BALF could directly reflect the inflammatory changes in the mice. To further appraise the extent of inflammation in the mice pulmonary tissues, we determined the protein concentration in BALF by BCA in order to reflect the permeability of endothelial cells and epithelial cells. The neutrophil number and protein content of BALF increased significantly with LPS stimulation, with an increase in the permeability of the endothelial and epithelial cells. After the administration of normal hUC-MSCs, the neutrophil number and protein concentration BALF reduced, indicating alleviation of inflammation in the experimental mice. After the administration of HP-hUC-MSCs, the neutrophil number and protein concentration in BALF reduced significantly. The inflammation in the lung was further reduced, indicating a significant statistical difference (Fig. 4c-d).

In the control group, the lungs of the mice were well inflated, and there was no hemorrhage on the surface. At each time point for the ALI model mice, the lung volume increased with an obvious edema,

and focal hemorrhages were detected on the lung surface. The microscopic observation revealed the infiltration of a large number of inflammatory cells, widening of the pulmonary interstitium, the collapse of the alveoli, pulmonary capillary congestion, hemorrhage, and other pathological changes, which manifested in ALI treatment group. By contrast, the normal hUC-MSCs treatment group showed less edema, bleeding, and congestion. The HP-hUC-MSCs experiment group highly reduced above pathological changes. No statistical difference between the CoCl₂ preconditioned hUC-MSCs group and hypoxia incubator-treated hUC-MSCs group (Fig. 4e).

After LPS, the levels of sTREM-1 and TNF- α in BALF increased relative to those of the control group, while the level of IL-10 decreased. After transplantation of hUC-MSCs, the level of IL-10 in BALF increased, while the concentration of sTREM-1 and TNF- α decreased, which together indicated that the inflammation in the ALI model mice was alleviated by hUC-MSCs. hUC-MSCs exhibited a repairing effect on the ALI mice. The HP-hUC-MSCs treatment group significantly improved the above-mentioned inflammatory and anti-inflammatory factors. Furthermore, serum concentrations of sTREM-1, TNF- α , and IL-10 followed the same trend as BALF, although the absolute concentration was significantly lower than those in BALF, implying that the inflammatory injury in other parts was much lighter than that in the lungs. This finding further validates the feasibility of our method to construct the ALI model using LPS (Fig. 4f).

In the LPS model group, the apoptosis of lung tissue increased, as manifested by increased expression of apoptotic proteins AKT, p-AKT, and PI3K, along with a reduction in the anti-apoptotic protein Bcl-2 expression. The normal hUC-MSCs could reverse the apoptosis of mouse lung tissues, as manifested by a decrease in the expression of the apoptosis proteins AKT, p-AKT, and PI3K, but an increase in the Bcl-2 expression, along with the reversal and repair effect of HP-hUC-MSCs on the mouse lung tissues that was stronger than that of normal hUC-MSCs. In addition, the changes in these genes in qPCR revealed the same trend in Western blotting. According to the findings, this process could be linked to the PI3K/AKT pathway. (Fig. 4g-h).

In LPS-induced ALI mice, hUC-MSCs can suppress TREM-1 expression

Our results confirmed that hUC-MSCs could limit TREM-1 expression in ALI mice mediated by LPS from 3 aspects of Western blotting, IHC, and qPCR, which has a significant impact on the the treatment of ALI.

In the IHC, 5 high-power fields ($\times 400$) were randomly selected from each section. Then, the area of positive objects under every high-power field was calculated utilizing Image-J software, reflecting the intensity of positive protein. As can be seen from the figure, the inflammatory cells including neutrophils, monocytes, and macrophages in the LPS group were strongly TREM-1 positive; the hUC-MSCs group was TREM-1 positive for a few scattered inflammatory cells, and the HP-hUC-MSCs group was positive for individual inflammatory cells. Moreover, no obvious difference was seen between the CoCl₂-pretreated hUC-MSCs group and hypoxia incubator-treated hUC-MSCs group (ns, $p > 0.05$) (Fig. 5a).

The level of TREM-1 in lung was dramatically elevated after LPS stimulation, according to Western blotting and qPCR data. (####, $p < 0.0001$). After the administration of normal hUC-MSCs, TREM-1 expression was significantly reduced, showing a statistical difference (****, $p < 0.0001$); after the administration of HP-hUC-MSCs, the expression of TREM-1 was further decreased, demonstrating that the difference is statistically significant (****, $p < 0.0001$) (Fig. 5b-d).

Individuals with severe pneumonia had significantly higher concentration of sTREM-1 in their serum

A sample of 40 individuals were hospitalized to Jilin University's Second Hospital of the Jilin University from June–December 2021 enrolled in this study. The 24 patients with severe pneumonia included 13 men and 11 women of an average age of 67 ± 14 years. The 16 patients of common pneumonia included 10 men and 6 women of an average age of 64 ± 5 years. The 10 healthy controls included 4 men and 6 women of an average age 62 ± 4 years. No significant difference was noted in the age and gender among the 3 groups ($p > 0.05$). This study was conducted after obtaining informed consent from the patients before blood collection. (Fig. 6)

hUC-MSCs protect ALI mice from lung injury by inhibiting TREM-1 expression.

To achieve the dry weight, we first determined the lungs' wet weight and then baked them for 48 hours at 60°C . The W/D value was calculated to determine the severity of pulmonary edema in each group of mice. We also examined the MPO of the lung tissues to assess the degree of inflammatory cells infiltration and migration. The results indicated that the W/D and MPO of the lungs increased significantly in the LRS + LPS group. LR12 is a synthetic inhibitor of TREM-1. After the administration of LR12 or normal hUC-MSCs, the W/D and MPO of the lung evidently decreased, showing a statistical difference. This level decreased further, and a statistically significant difference was noted after the administration of LR12 and normal hUC-MSCs. The results showed that hUC-MSCs could reduce the W/D and MPO of ALI mice by inhibiting the expression of TREM-1 (Fig. 7a-b).

BALF is an important marker for evaluating lung functions, while the total number of cells in BALF, particularly neutrophils, directly reflected the inflammatory changes in mice. To get a better idea of how much inflammation there is in mice's lungs, we determined the protein concentration in BALF by BCA to reflect the permeability of the endothelial and epithelial cells. In BALF, the number of neutrophils, all cells, and protein content all rose significantly in the LRS + LPS group along with an increase in the permeability of endothelial and epithelial cells. After the administration of LR12 or normal hUC-MSCs, the neutrophil number, overall cells, and protein content in BALF lowered, indicating improvement in inflammation in the experimental mice. After the administration of LR12 and normal hUC-MSCs, the neutrophil number, complete cells, and protein concentration in BALF diminished significantly. The inflammation in the lungs reduced further, and there was a significant statistical difference. Our results showed that hUC-MSCs could reduce the neutrophil number, cumulative cells, and protein content in BALF by inhibiting the expression of TREM-1 (Fig. 7c-e).

The mice's lungs were well inflated in the control mice, and there was no hemorrhage on the surface. At each time point in the LRS + LPS group, the lung volume increased with obvious edema, and focal hemorrhages were noted on the lung surface. The microscopic observation showed the infiltration of a large number of inflammatory cells, widened pulmonary interstitium, collapsed alveoli, pulmonary capillary congestion, hemorrhage, and other pathological changes mainly manifested in the LRS + LPS mice. In contrast, the normal hUC-MSCs or the LR12-treatment group showed less edema, bleeding, and congestion. The normal hUC-MSCs and LR12 treatment group significantly reduced the abovementioned pathological changes. As noted above, results indicated that by decreasing TREM-1 expression, hUC-MSCs alleviated ALI mice with lung inflammation. (Fig. 7f).

In IHC, 5 high-power fields ($\times 400$) were randomly selected from each section. The area of positive objects under every high-power field was calculated using Image-J application, reflecting the intensity of positive protein. As can be seen from the figures, the inflammatory cells, including neutrophils, monocytes, and macrophages, in the LRS + LPS group were strongly TREM-1 positive; the LR12 + LPS group and LRS + LPS + hUC-MSCs group was TREM-1 positive for a few scattered inflammatory cells, and the LR12 + LPS + hUC-MSCs group was positive for individual inflammatory cells. These values indicated that the administration of LR12 or hUC-MSCs could significantly diminish TREM-1 expression in ALI mice. Moreover, LR12 and hUC-MSCs could synergistically suppress TREM-1 expression of in ALI mice (Fig. 7g).

In the LRS + LPS group, the levels of sTREM-1 and TNF- α in the lung tissues, serum, and BALF risen relative to those in the control mice, albeit IL-10 level declined. After the transplantation of hUC-MSCs or LR12, IL-10 concentration in lung tissues, serum, and BALF increased, while the concentration of sTREM-1 and TNF- α decreased, indicating that the inflammation was alleviated by hUC-MSCs or LR12. hUC-MSCs or LR12 exhibited a repairing effect on ALI mice. The LR12 + LPS + hUC-MSCs group significantly improved the abovementioned inflammatory and anti-inflammatory factors. These results also indicate that by reducing TREM-1 expression, hUC-MSCs were able to reduce lung inflammation in ALI animals. Further, Zhu J Q et al. found that MSCs reduce ALI damage generated by LPS-induced by suppressing Ly6C⁺ CD8⁺ T cells' pro-inflammatory activity^[12]. (Fig. 7h).

The therapeutic impact of hUC-MSCs in mice with LPS-caused ALI was associated with TREM-1-regulated TLR4 and MyD88

When comparison to the control group, TREM-1, TLR4, and MyD88 expression in the LRS + LPS mice were greatly upregulated ($p < 0.001$). When compared to the LRS + LPS mice, the LR12 + LPS and LRS + LPS + hUC-MSCs groups showed inhibition in TREM-1, TLR4, and MyD88 expression, showing an obvious statistical difference ($p < 0.001$). By contrast, TREM-1, TLR4, and MyD88 expression levels were considerably lower in the LR12 + LPS + hUC-MSCs group ($p < 0.05$), demonstrating that TREM-1-mediated expression of TLR4 and MyD88 was relevant to the protective role of hUC-MSCs against ALI (Fig. 8a-b).

The therapeutic impact of hUC-MSCs in mice with LPS-caused ALI was connected to TREM-1-regulated PI3K/Akt phosphorylation

When compared with the control group, the expressions of p-PI3K and p-Akt in the LRS + LPS group upregulated, and there was a statistical difference ($p < 0.05$). When contrasted with the LRS + LPS mice, LR12 + LPS and LRS + LPS + hUC-MSCs groups showed significant inhibition in p-PI3K and p-AKT expression, and displayed an obvious statistical difference between them ($p < 0.001$). In contrast, the LR12 + LPS + hUC-MSCs group exhibited a stronger effect on reducing p-PI3K and p-AKT levels, demonstrating a substantial distinction among them ($p < 0.05$). These results indicated that the preventive impact of hUC-MSCs on LPS-caused ALI correlated with PI3K/Akt phosphorylation level through TREM-1 (Fig. 9).

Discussion

hUC-MSCs have various benefits over adult MSCs, which are an emerging field with promising applications for managing severe COVID19^[13-14]. They offer the absolute advantages of low immunogenicity, convenient access, and no ethical issues, making them a rising star in cell therapy. However, the value of hUC-MSCs is not restricted to severe COVID19 along but also to the treatment of ALI/ARDS caused by various reasons. Severe pneumonia, as a typical representative of ALI/ARDS, was considered as the research object in the present study. Severe pneumonia is a common clinical infectious disease of the respiratory system that can trigger a strong immune response, produce a large number of inflammatory mediators, leading to the damage of organ functions, and even multiple organ failure, which ultimately aggravates the progression of the disease. TREM-1 plays a significant role in respiratory infections and sepsis pathogenesis^[15]. The concentration of sTREM-1 in the plasma of the severe pneumonia cohort was massively greater than that of the normal pneumonia and control subjects, with a big difference amongst them ($p < 0.05$), which was consistent with the results of past studies^[16-18].

To see if hUC-MSCs have some impact on BEAS-2B, we co-cultured hUC-MSCs or HP-hUC-MSCs with BEAS-2B under LPS stimulation and then examined the apoptosis of BEAS-2B. Our results showed that hUC-MSCs and HP-hUC-MSCs could reverse the BEAS-2B apoptosis of BEAS-2B. Similarly, hUC-MSCs decreased the level of caspase-3 in a hypoxic-ischemic encephalopathy model^[19]. The HP-UC-MSCs exhibited a stronger reverse repair effect than normal hUC-MSCs. hUC-MSCs have previously been proven to relieve alveolar epithelial cells- (AEC II) apoptosis in sepsis-induced ALI^[20]. However, unlike in our study, the co-culture of hUC-MSCs and A549 was adopted in this past study. In our study, we initially used A549 and hUC-MSCs co-culture. However, the results showed that hUC-MSCs did not repair the A549 induced by LPS, rather they further reduced the viability of A549. The results of the Western blotting analyses revealed that the expression of an apoptotic protein (AKT) increased in the co-culture group of A549 and hUC-MSCs when compared to that in the LPS mice, albeit anti-apoptotic protein (Bcl-2) expression to be less expressed. Therefore, we believe that it is reasonable to think that in our investigation, hUC-MSCs were unable to prevent A549 apoptosis triggered by LPS. On one hand, the

reason for this may be that A549 is a lung adenocarcinoma cell line with tumor characteristics. In order to inhibit the growth of tumor cells, hUC-MSCs increased the apoptosis of A549, which, however, may be related to the stimulating concentration of LPS. In our study, the LPS concentration was 1 ug/mL, while the LPS concentration in the abovementioned literature was 20 ug/mL. Therefore, we finally adopted the co-culture of BEAS-2B with hUC-MSCs in the present study.

In this study, through intratracheal instillation, LPS was used to construct an ALI model. This method could adequately simulate the disease process of ALI in patients, and the degree of ALI could be easily controlled. LPS could cause local damage in the lungs and not induce systemic inflammatory response and organ failure. The present results revealed that other than the lungs, such as the heart, liver, spleen, and kidney, did not show inflammatory cells' infiltration or any LPS-induced abnormal function, indicating that the method of constructing the ALI model in this study was successful and feasible. We also conducted a series of biochemical tests, including HE and IHC, among others. Our results showed that hUC-MSCs and HP-hUC-MSCs have the potential to lower lung W/D ratios as well as neutrophil migration and infiltration, which finally manifested as the inhibition of MPO vitality. MPO, a ROS generator, its reduction has a positive correlation with the inhibition of BAX with pro-apoptotic function [21]. Pathological observation in HE indicated that hUC-MSCs and HP-hUC-MSCs could effectively protect the lung tissue structure, and improve pulmonary hemorrhage, edema, and inflammatory infiltration. hUC-MSCs exhibited a preventive role against ALI mice provoked LPS as well as an enhanced effect of HP-hUC-MSCs.

TREM-1 is just a recently identified immunoglobulin protein that is linked to inflammation and displayed on the membrane of myeloid cells including neutrophils, mature monocytes, and macrophages. As an important marker of inflammatory diseases, it exhibits a good correlation with the severity of infection [22-23]. Several studies across the world have confirmed that sTREM-1 showcases important clinical significance for the early diagnosis, disease assessment, and prognosis of pneumonia, with high sensitivity and specificity [24-26]. The present results revealed that, in the LRS + LPS group, when comparison to the normal control mice, TLR4, MyD88, p-PI3K, and p-Akt expression in the lung tissues was significantly upregulated, indicating that the TLR4/MyD88 and PI3K/AKT regulatory pathways involved in the LPS-generated ALI model. When compared to the LRS + LPS mice, TLR4, MyD88, p-PI3K, and p-AKT expression in the TREM-1 inhibition and hUC-MSCs treatment mice was tremendously decelerated, indicating that inhibition of the TREM-1 expression can, in turn, inhibit the expression of TLR4 and MyD88 as well as the phosphorylation of PI3K/AKT, which together inhibit LPS-induced inflammatory response in ALI mice. When compared with the TREM-1 inhibition group, the hUC-MSCs treatment group exhibited a significantly stronger effect on reducing the levels of TLR4, MyD88, p-PI3K, and p-AKT, suggesting that inhibiting the expression of TREM-1 can only partially explain the mechanism in the treatment of ALI by hUC-MSCs. Further research on the mechanisms is warranted. Although we could not directly prove their relationship, our findings support that the TLR4/MyD88 and PI3K/AKT phosphorylation signaling pathways may partially mediate the protective efficacy of hUC-MSCs in LPS-

produced ALI mice. The findings of our study offer a new therapy option for ALI. Figure 10 depicts the likely mechanism of hUC-MSCs in the therapy of ALI.

hUC-MSCs can exert anti-inflammation and anti-apoptosis effect on ALI or LPS-induced BEAS-2B injury by reducing TREM-1 expression, which perhaps linked to the TLR4/MyD88 pathway and the phosphorylation of PI3K/Akt.

Conclusion

Ultimately, our studies discovered that HP-hUC-MSCs can exert a stronger therapeutic effect when compared with hUC-MSCs on ALI by reducing TREM-1 expression, which is perhaps associated with the TLR4/MyD88 pathway and the phosphorylation of PI3K/Akt.

Abbreviations

ALI/ARDS

Acute lung injury/acute respiratory distress syndrome

COVID19

Corona Virus Disease 2019

hUC-MSCs

human umbilical cord mesenchymal stem cells

HP-hUC- MSCs

Hypoxic preconditioning umbilical cord mesenchymal stem cells

W/D

wet/dry

BALF

broncho- alveolar lavage fluid

GC

glucocorticoids

CCK8

Cell Counting Kit-8

ELISA

Enzyme-link ed immunosorbent assay

HE

Hematoxylin and Eosin

MPO

Myeloperoxidase

LPS

Lipopoly- saccharide

IHC

Immunohistochemistry

sTREM-1

soluble triggering receptor expressed on myeloid cells

TREM-1

triggering receptor expressed on myeloid cells. AECII:Alveolar epithelial cells-

Declarations

Ethics approval and consent to participate

The study was conducted in strict accordance with the recommendations of the Guide for the Care and Use of Laboratory Animals from the National Institutes of Health. All protocols were approved by the Institutional Animal Care and Use Committee of the Second Hospital of Jilin University.

Consent for publication

Not applicable.

Availability of data and materials

The data that support the findings of this study are available from corresponding author upon reasonable request.

Competing interests

The authors declared no potential conflicts of interest.

Funding

This study was funded by the Department of Finance of Jilin Province (Grant NO. 2020SC2T005).

Authors' contributions

Yujuan Wang and Junling Yang contributed to the conception and writing of this review. All authors have reviewed and approved the submitted work.

Acknowledgements

Thanks for the editorial work of Editage Ltd. Thanks to Changchun Sigma Company for donating hUC-MSCs.

References

1. Bakowitz M, Bruns B, McCunn M. Acute lung injury and the acute respiratory distress syndrome in the injured patient. *Scand J Trauma Resusc Emerg Med.* 2012;20:54.

2. Hayes M, Curley G, Ansari B, et al. Clinical review: Stem cell therapies for acute lung injury/acute respiratory distress syndrome—hope or hype? *Crit Care*. 2012;16:205.
3. Chacko B, Peter JV, Tharyan P, John G, et al. Pressure-controlled versus volume-controlled ventilation for acute respiratory failure due to acute lung injury (ALI) or acute respiratory distress syndrome (ARDS). *Cochrane Database Syst Rev*. 2015;1:CD008807.
4. Hu X, Liu L, Wang Y, Yu Y, Li Z, Liu Y, Chai J. Human Umbilical Cord-Derived Mesenchymal Stem Cells Alleviate Acute Lung Injury Caused by Severe Burn via Secreting TSG-6 and Inhibiting Inflammatory Response. *Stem cells international*; 2022. p. 8661689.
5. Fernández-Francos S, Eiro N, González-Galiano N, Vizoso FJ. Mesenchymal Stem Cell-Based Therapy as an Alternative to the Treatment of Acute Respiratory Distress Syndrome: Current Evidence and Future Perspectives. *International journal of molecular sciences*, 2021, 22(15), 7850.
6. Chu K-A, Yeh C-C, Kuo F-H, Lin W-R, Hsu C-W, Chen T-H, Fu Y-S. Comparison of reversal of rat pulmonary fibrosis of nintedanib, pirfenidone, and human umbilical mesenchymal stem cells from Wharton's jelly. *Stem Cell Res. Ther.* 2020;11.
7. Dao MA, Pepper KA, Nolta JA. Long-term cytokine production from engineered primary human stromal cells influences human hematopoiesis in an in vivo xenograft model. *Stem Cells*. 1997; 15:443–454.
8. Nolta JA, Hanley MB, Kohn DB. Sustained human hematopoiesis in immunodeficient mice by cotransplantation of marrow stroma expressing human interleukin-3: Analysis of gene transduction of long-lived progenitors. *Blood*. 1994;83:3041–51.
9. Pittenger MF, Mackay AM, Beck SC, et al. Multilineage potential of adult human mesenchymal stem cells *Science*. 1999;284:143–7.
10. Dominici M, Le Blanc K, Mueller I, et al. Minimal criteria for defining multipotent mesenchymal stromal cells The International Society for Cellular Therapy position statement. *Cytotherapy*. 2006; 8:315–7.
11. Wang C, et al. Interleukin-10-overexpressing mesenchymal stromal cells induce a series of regulatory effects in the inflammatory system and promote the survival of endotoxin-induced acute lung injury in mice model. *DNA Cell Biol*. 2018;37(1):53–61.
12. Zhu J, Feng B, Xu Y, et al. Mesenchymal stem cells alleviate LPS-induced acute lung injury by inhibiting the proinflammatory function of Ly6C + CD8 + T cells. *Cell Death Dis*. 2020;11(10):829.
13. Wei L, Zhang L, Yang L, et al. Protective Effect of Mesenchymal Stem Cells on Isolated Islets Survival and Against Hypoxia Associated With the HIF-1 α /PFKFB3 Pathway. *Cell Transplant*. 2022;31:9636897211073127.
14. Coelho A, Alvites RD, Branquinho MV, et al. Mesenchymal Stem Cells (MSCs) as a Potential Therapeutic Strategy in COVID-19 Patients: Literature Research. *Front Cell Dev Biol*. 2020 Nov;19:8:602647.
15. Feng JY, Su WJ, Chuang FY, et al. TREM-1 enhances Mycobacterium tuberculosis-induced inflammatory responses in macrophages. *Microbes Infect*. 2021;23(1):104765.

16. Tejera A, Santolaria F, Diez ML, et al. Prognosis of community acquired pneumonia (CAP): value of triggering receptor expressed on myeloid cells-1 (TREM-1) and other mediators of the inflammatory response. *Cytokine*. 2007;38(3):117–23.
17. Chen XS. The relationship between the level of PCT, RAGE, sTREM-1 in serum and the severity and prognosis of severe pneumonia patients. *Labeled Immunoass Clin*. 2020;27(1):6.
18. Nong XG, Cheng WP. The diagnostic value of neutrophil CD64 and sTREM-1 in serum of elderly community-acquired pneumonia. *Chin J Immunol*. 2016;32(6):4.
19. Xu J, Feng Z, Wang X, et al. hUC-MSCs Exert a Neuroprotective Effect via Anti-apoptotic Mechanisms in a Neonatal HIE Rat Model. *Cell Transpl*. 2019;28(12):1552–59.
20. Liu J. Inhibition of MEK/ERK signaling pathway by human umbilical cord blood-derived mesenchymal stem cells (hUC-MSC) reduces apoptosis of alveolar type II epithelial cells in sepsis-induced acute lung injury. Sun Yat-Sen University; 2016.
21. Hong SY, Teng SW, Lin W, et al. Allogeneic human umbilical cord-derived mesenchymal stem cells reduce lipopolysaccharide-induced inflammation and acute lung injury. *Am J translational Res*. 2020;12(10):6740–50.
22. Gibot S, Cravoisy A. Soluble Form of the Triggering Receptor Expressed on Myeloid Cells-1 as a Marker of Microbial Infection. *Clin Med Res*. 2004;2(3):181–7.
23. Bouchon A, Facchetti F, Weigand MA, et al. TREM-1 amplifies inflammation and is a crucial mediator of septic shock. *Nature*. 2001;410(6832):1103–7.
24. Ruiz-González A, Esquerda A, Falguera M, et al. Triggering receptor (TREM-1) expressed on myeloid cells predicts bacteremia better than clinical variables in community-acquired pneumonia. *Respirology*. 2011;16(2):321–5.
25. Porfyridis I, Plachouras D, Karagianni V, et al. Diagnostic value of triggering receptor expressed on myeloid cells-1 and C-reactive protein for patients with lung infiltrates: an observational study. *BMC Infect Dis*. 2010;10(1):286.
26. Zhang HF, Zhang X, Sha YX, et al. Value of sTREM-1 in serum and bronchoalveolar lavage fluid, APACHE II score, and SOFA score in evaluating the conditions and prognosis of children with severe pneumonia. *Chin J Contemp Pediatr*. 2020;22(6):626–31.

Figures

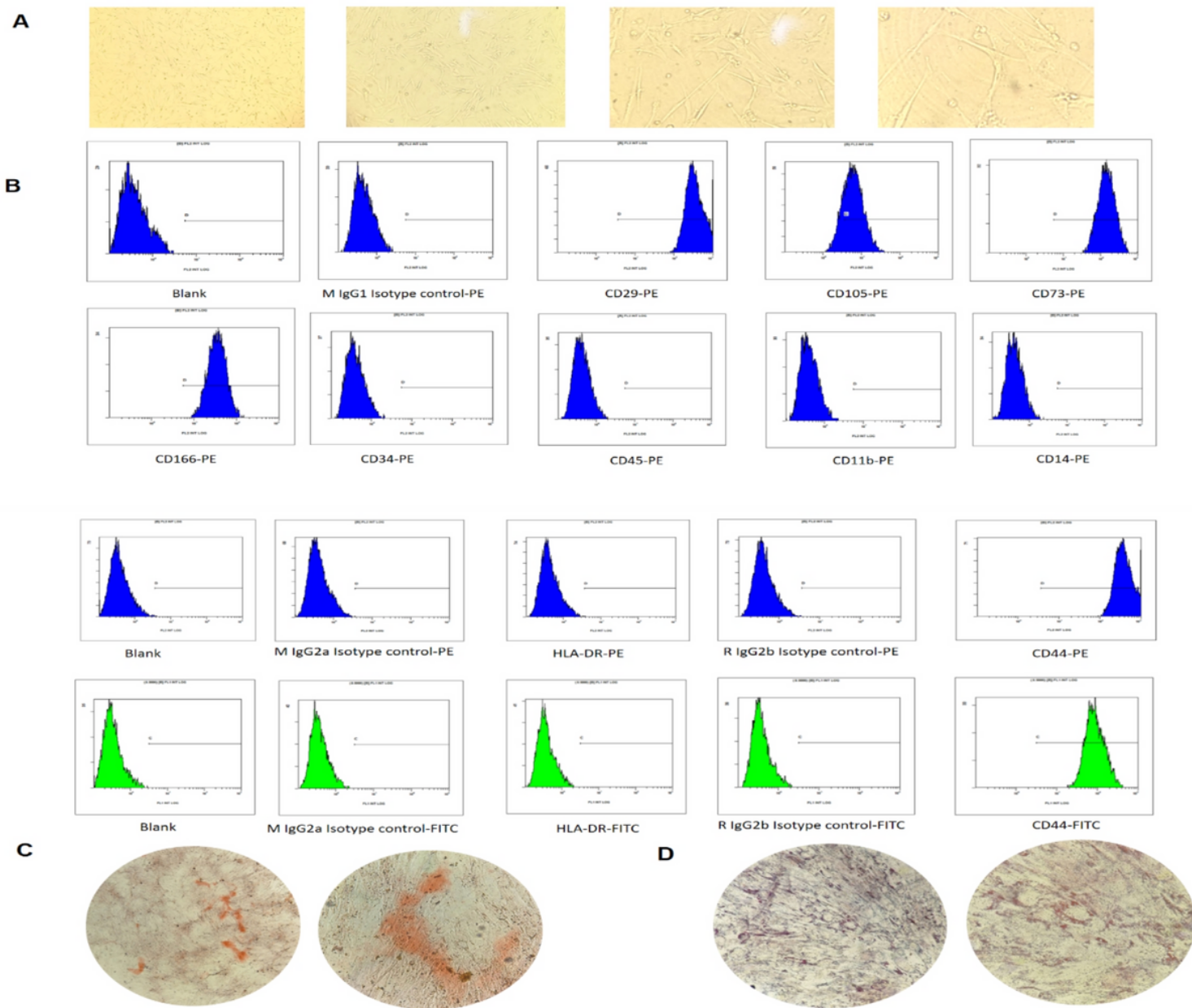


Figure 1

Characterization of hUC-MSCs. (a) Inverted microscopy revealed the morphology of hUC-MSCs at P3 cultured after 24 h as spindle-shaped and fibroblast-like. (b) The flow cytometer was used to detect the CD markers of hUC-MSCs. (c) hUC-MSCs osteogenesis revealed the formation of a calcified nodule. (d) hUC-MSCs adipogenesis revealed red-stained lipid droplets.

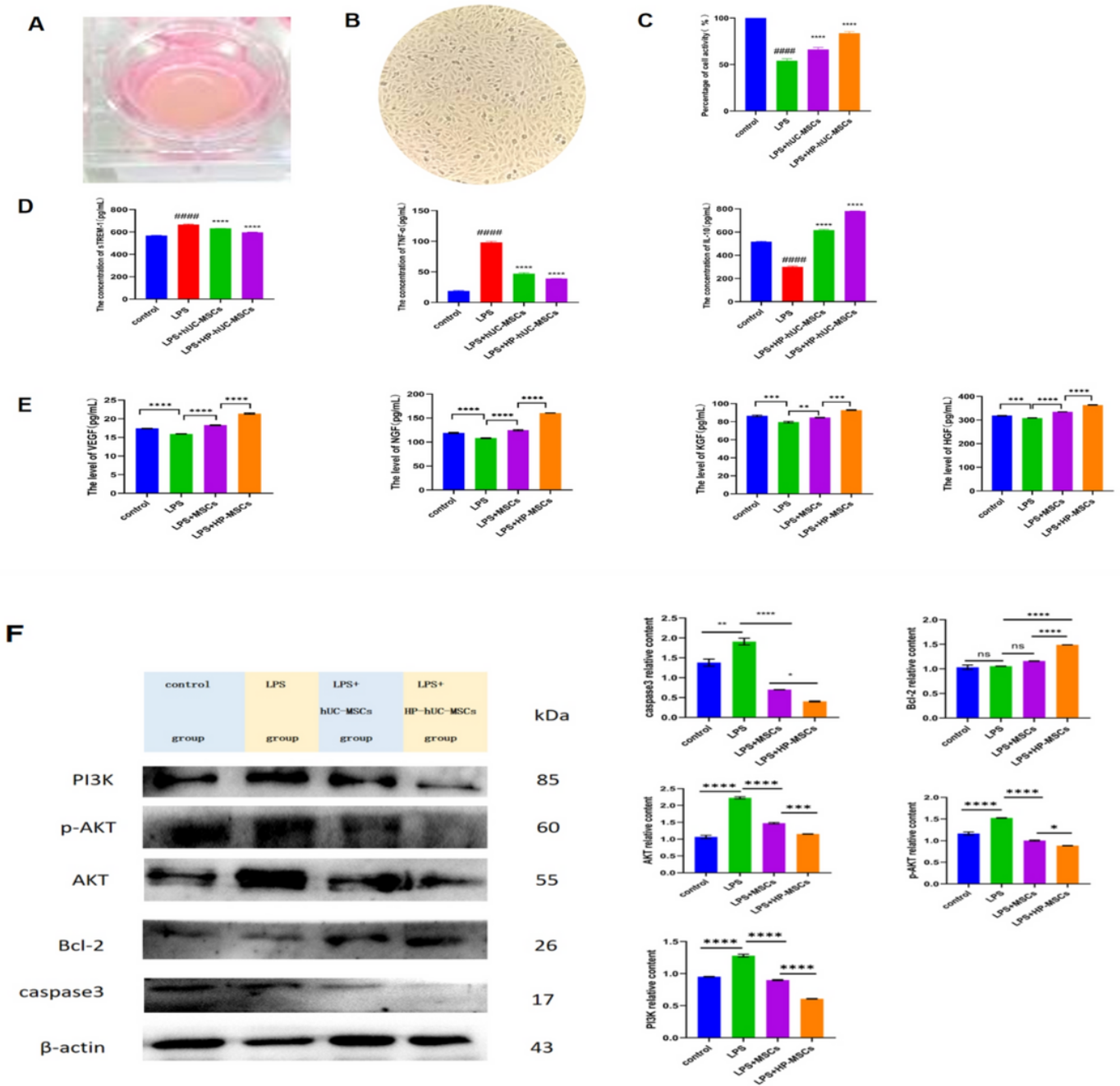


Figure 2

Co-culture of BEAS-2B with hUC-MSCs. (A) The Transwell chamber was suspended and used with 6-well plates. (B) Morphology of BEAS-2B cells under the microscope. (C) CCK8 was used to detect the vitality of BEAS-2B. (D) hUC-MSCs could alleviate BEAS-2B inflammatory injury by regulating the anti-inflammatory balance. (E) hUC-MSCs can participate in the repair process after BEAS-2B injury through the paracrine system. (F) hUC-MSCs can reduce apoptosis after BEAS-2B injury.

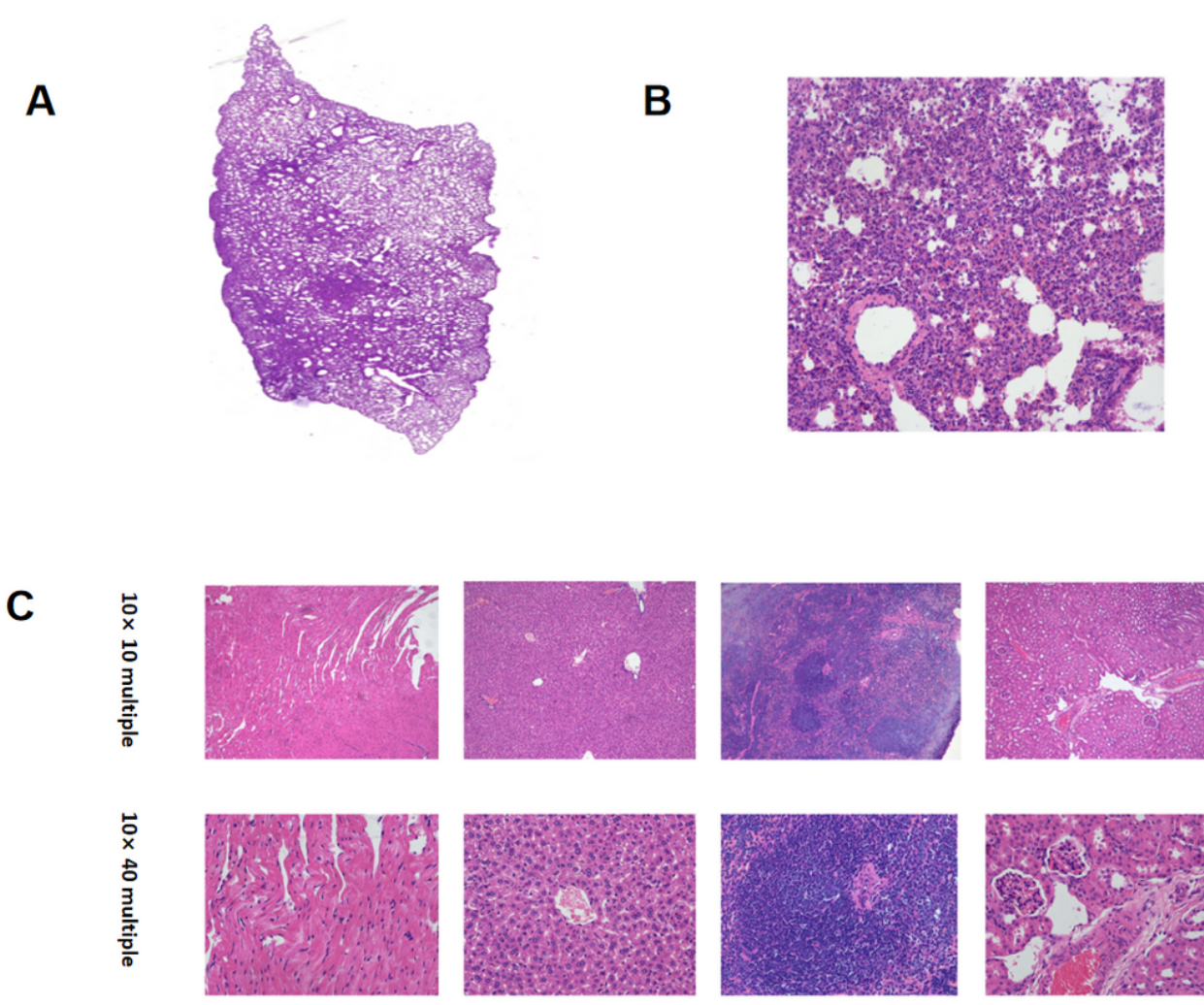


Figure 3

To make LPS-caused ALI mouse model. (A) The overall scan of the ALI model lung tissue section. (B) The image of the ALI model lung tissue section under the microscope (10x20). (C) The image of ALI model heart, liver, spleen, and kidney tissue sections under the microscope (10x10 multiple and 10x40 multiple).

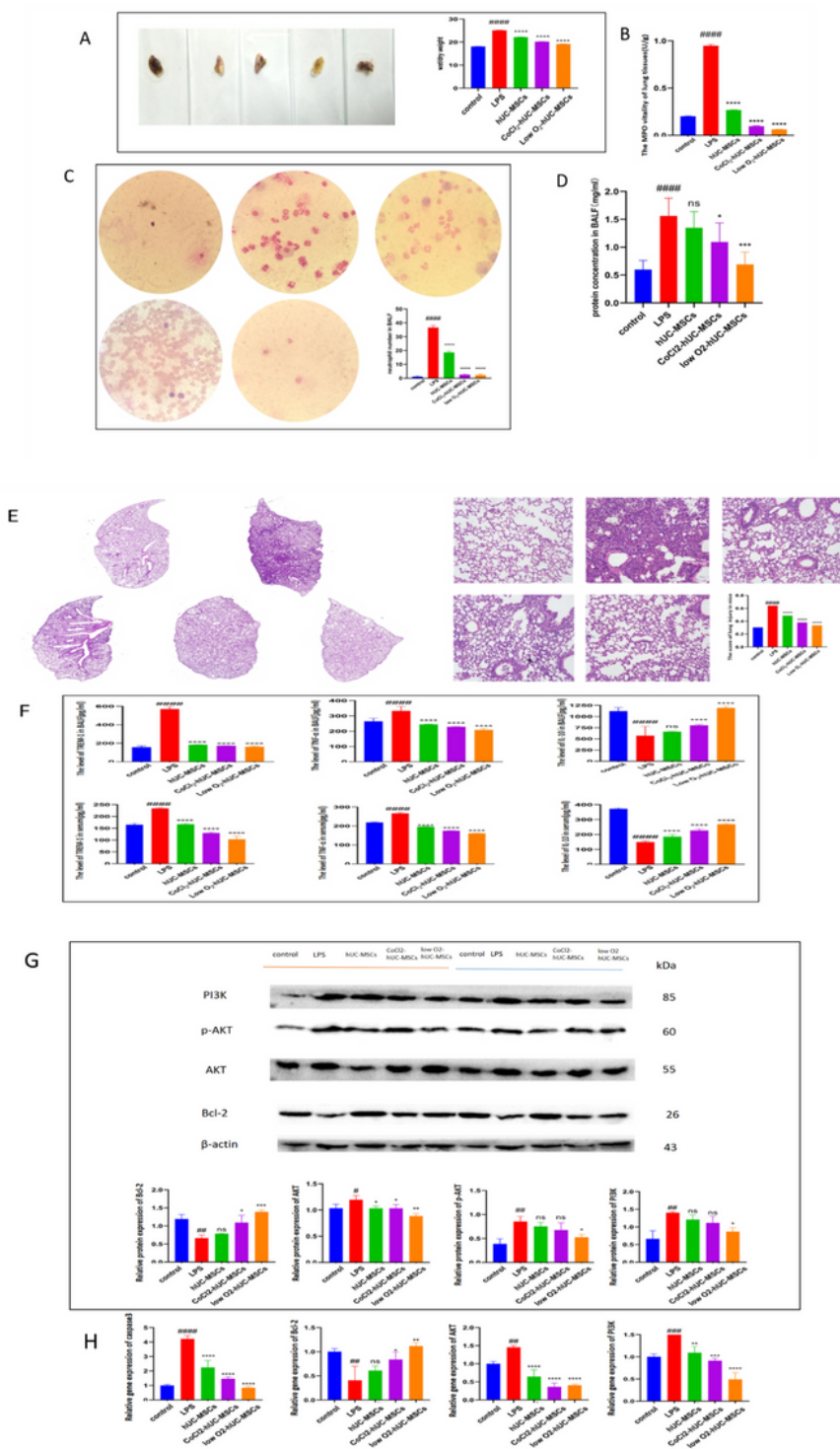


Figure 4

hUC-MSCs can improve ALI mice and HP-hUC-MSCs can boost their effectiveness. (A) The results of W/D. (B) The results of MPO in the lungs. (C) The changes in the neutrophil count in BALF. (D) The concentration of proteins in BALF. (E) The overall scan of the ALI model lung tissue section and the image of the ALI model lung tissue section under the microscope (10×20). (F) The concentration of TREM-1, TNF- α , and IL-10 in the mice BALF and serum. (G) Western blotting was used to evaluate the

protein expression of PI3K, p-AKT, AKT, and Bcl-2, and the statistical results of the Western blot are displayed in the pane. (H) The gene transcription of PI3K, caspase3, AKT, and Bcl-2 was detected by qPCR analysis. # $p < 0.05$ relative to the control group. * $p < 0.05$ relative to the LPS group. For multiple group comparisons, one-way ANOVA was used, complied with Tukey's post-hoc test.

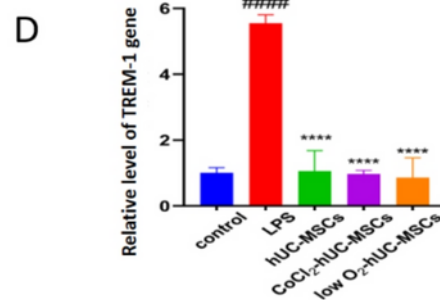
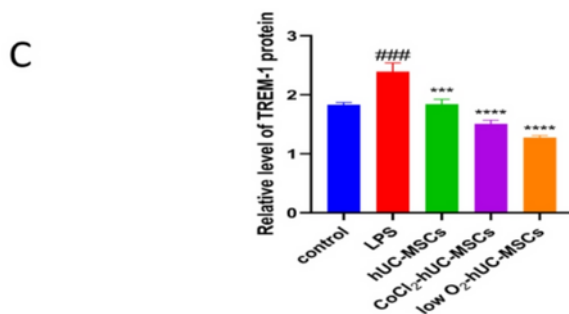
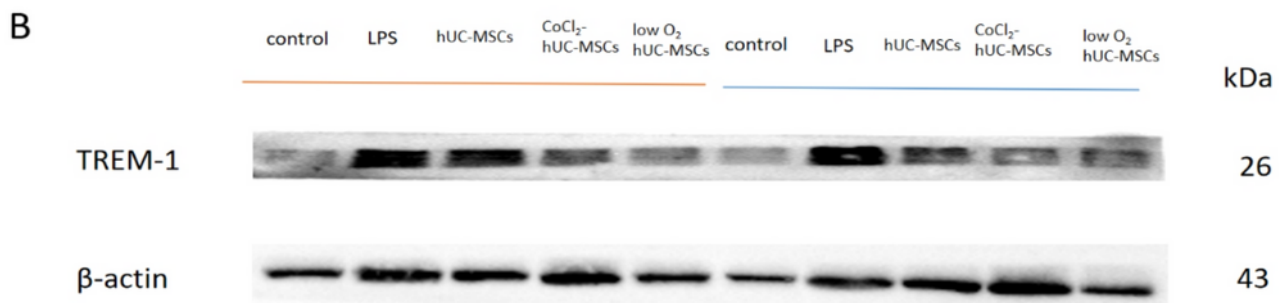
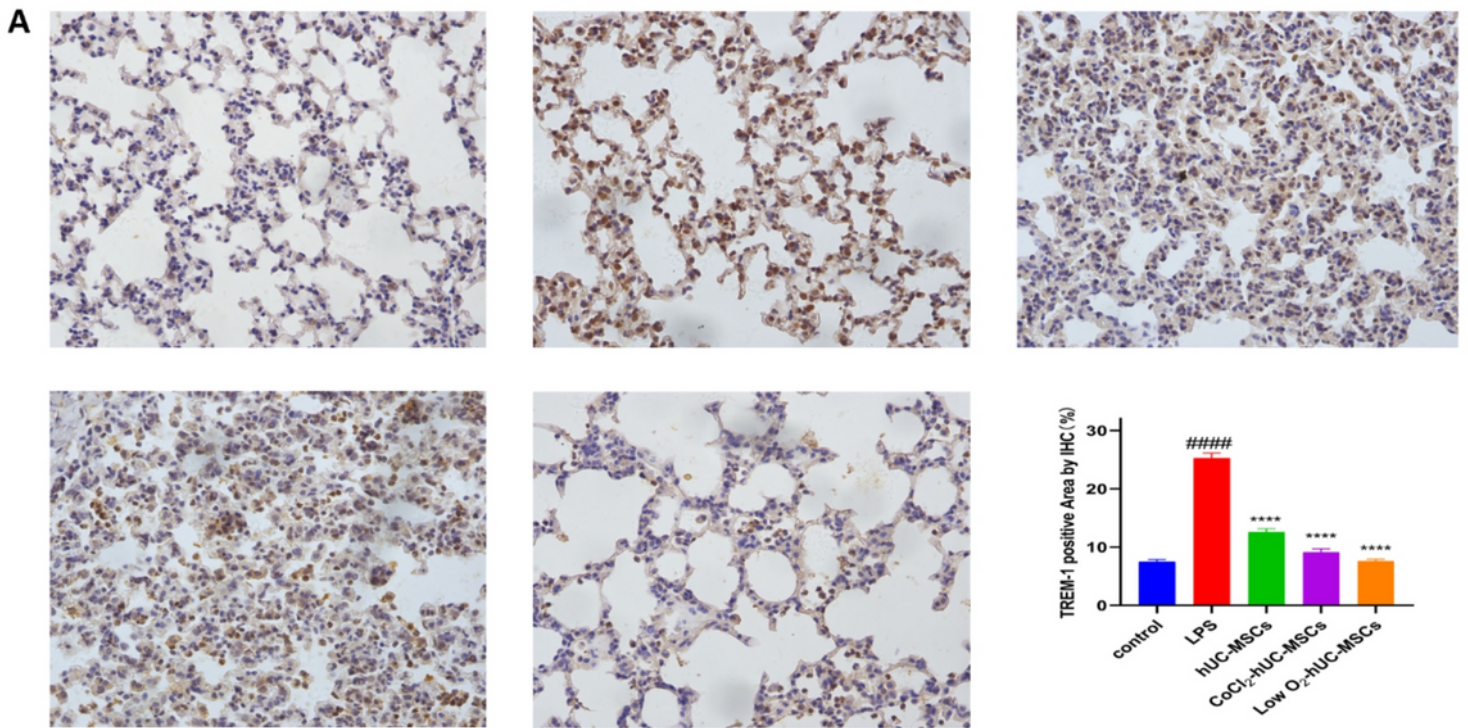


Figure 5

TREM-1 expression was inhibited by hUC-MSCs in the lung tissues of LPS-induced ALI animals. (A) TREM-1 protein expression was investigated using IHC and statistical methods. (B) TREM-1 protein expression was analyzed using Western blotting. (C) The pane displays the Western blotting quantitative measurements. (D) qPCR technique was used to evaluate TREM-1 gene transcription. #p < 0.05 relative to the control group. *p < 0.05 relative to the LPS group. For multiple group analyses, one-way ANOVA was used, complied by Tukey's post-hoc test. Three times the cellular experiment was carried out.

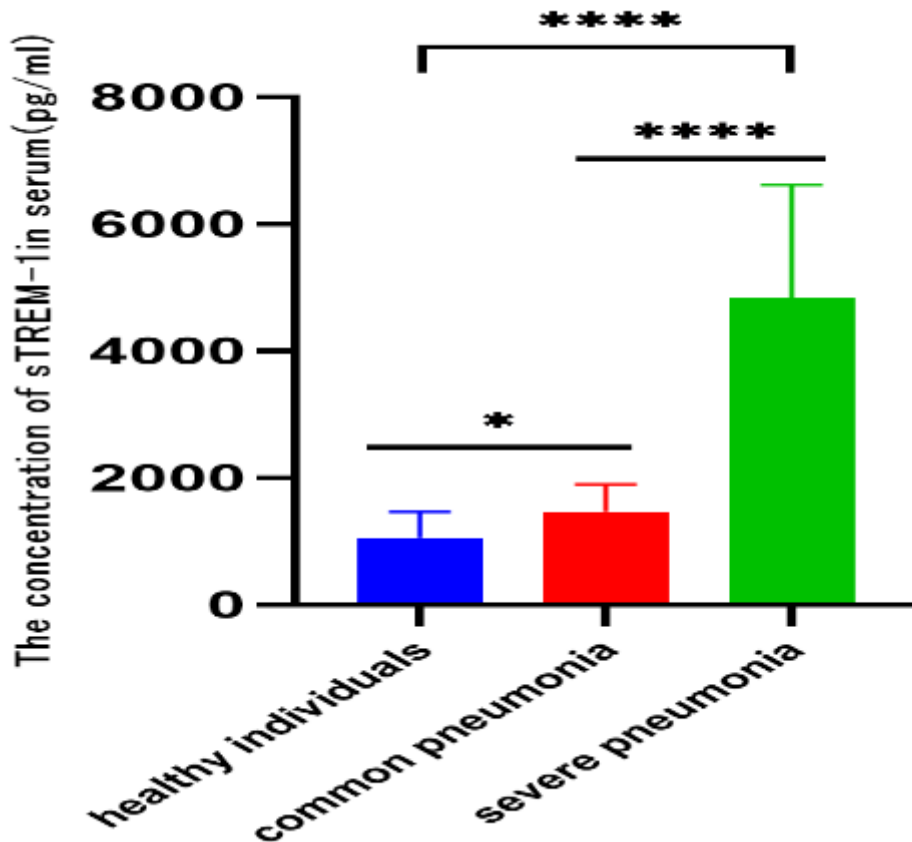


Figure 6

The concentration of sTREM-1 in the blood of patients in various groups. Cases of severe pneumonia had considerably greater levels of sTREM-1 in their serum than the control and ordinary pneumonia subgroups, indicating a substantial difference. (****, $p < 0.0001$); Patients with regular pneumonia had elevated amounts of sTREM-1 in their serum than those in the control group, representing a statistical difference. (*, $p < 0.05$).

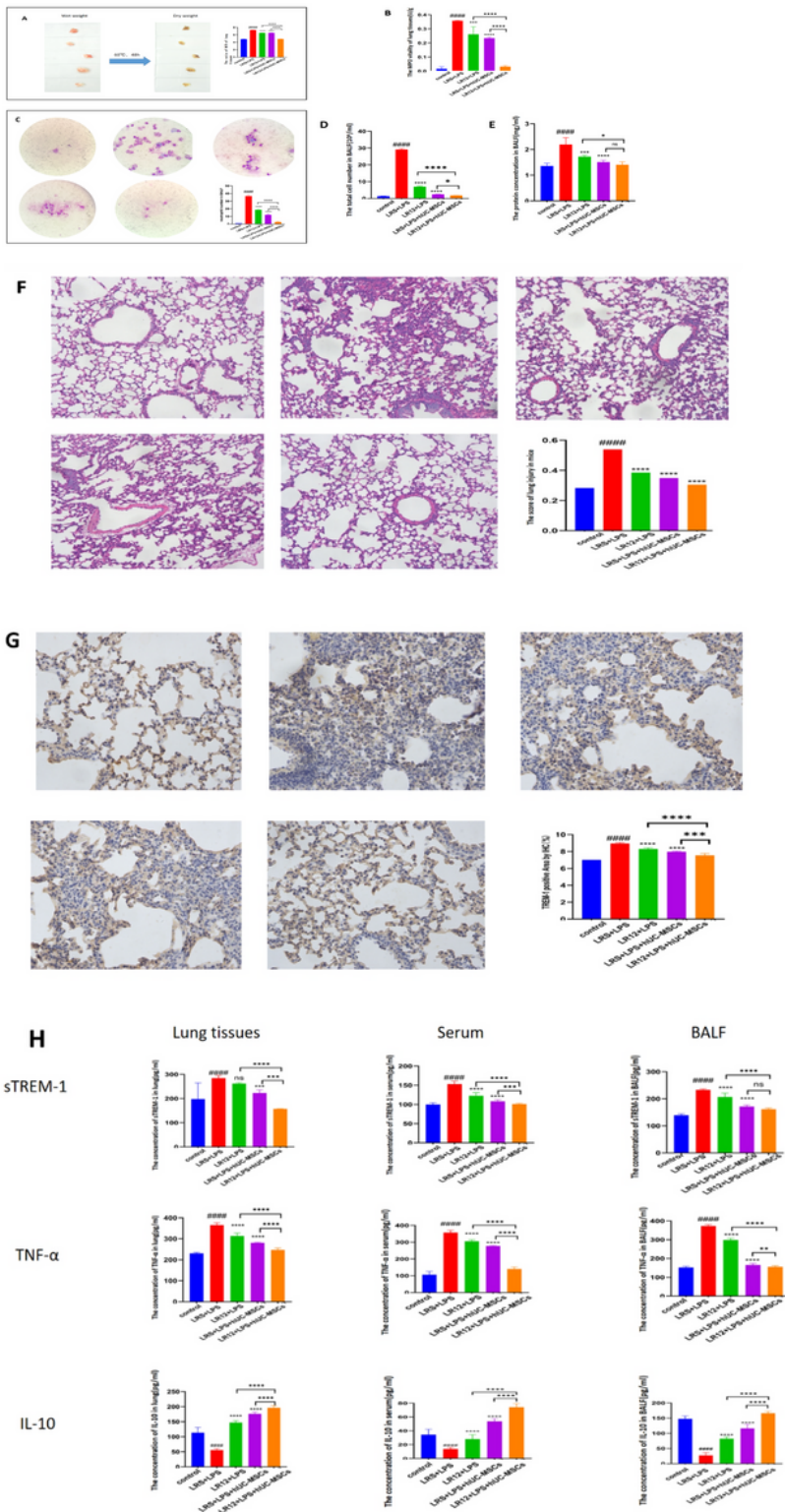


Figure 7

hUC-MSCs alleviate lung inflammation in ALI mice by inhibiting TREM-1 expression. (A) The wet and dry weight of the lungs and the statistical results of W/D. (B) The results of MPO in the lungs. (C) The change in the neutrophil count in mice BALF. (D) The total number of cells in mice BALF. (E) The concentration of protein in mice BALF. (F) The image of the lung tissue section in different groups as observed under the microscope (10 \times 20). (G) TREM-1 expression was examined through IHC analysis and statistical study.

(H) The concentration of TREM-1, TNF- α , and IL-10 in the lungs, serum, and BALF of mice. # $p < 0.05$ relative to the control mice. * $p < 0.05$ relative to the LRS+LPS mice.

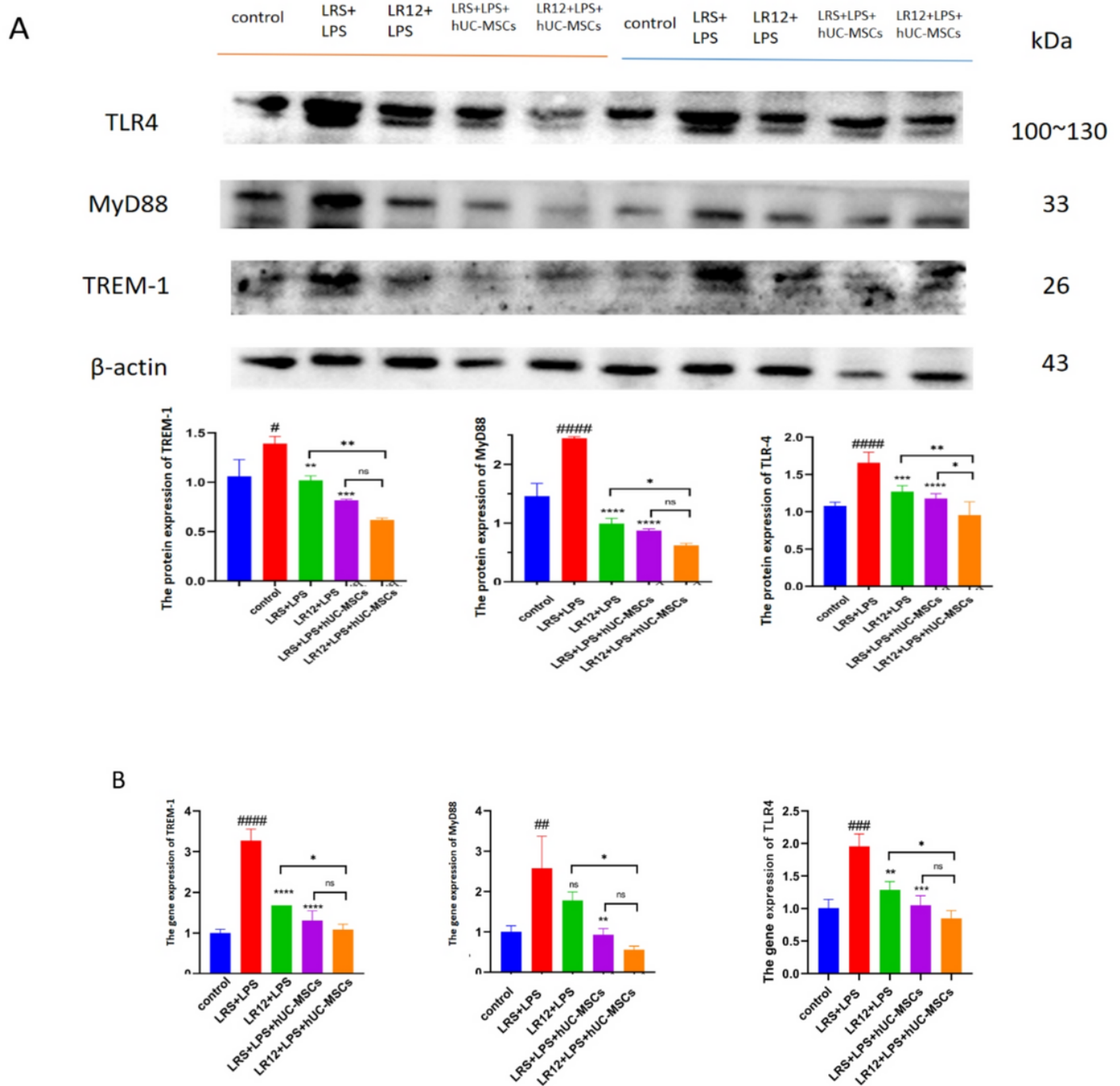


Figure 8

TREM-1, TLR4, and MyD88 protein and gene expression in mice. (A) Western blotting was used to assess TREM-1, MyD88, and TLR4 protein expression and corresponding statistical results shown in the pane. (B) TREM-1, MyD88, and TLR4 gene expression examined by qPCR. The internal standard for both

Western blotting and qPCR experiments was β -actin. # $p < 0.05$ relative to the control group. * $p < 0.05$ relative to the LRS+LPS group.

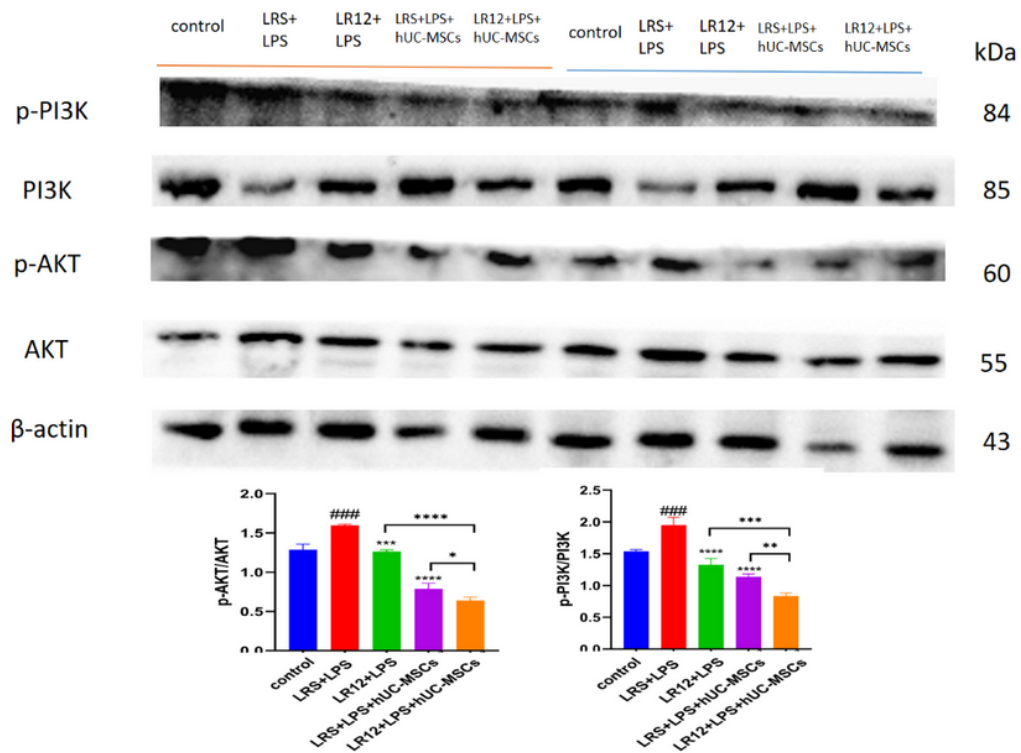


Figure 9

The protein expression of p-PI3K, PI3K, p-AKT, and AKT in the lung. Western blotting was used to evaluate the expression levels of p-PI3K, PI3K, p-AKT, and AKT, and the corresponding statistical findings displayed in the pane. # $p < 0.05$ relative to the control lung. * $p < 0.05$ relative to the LRS+LPS lung.

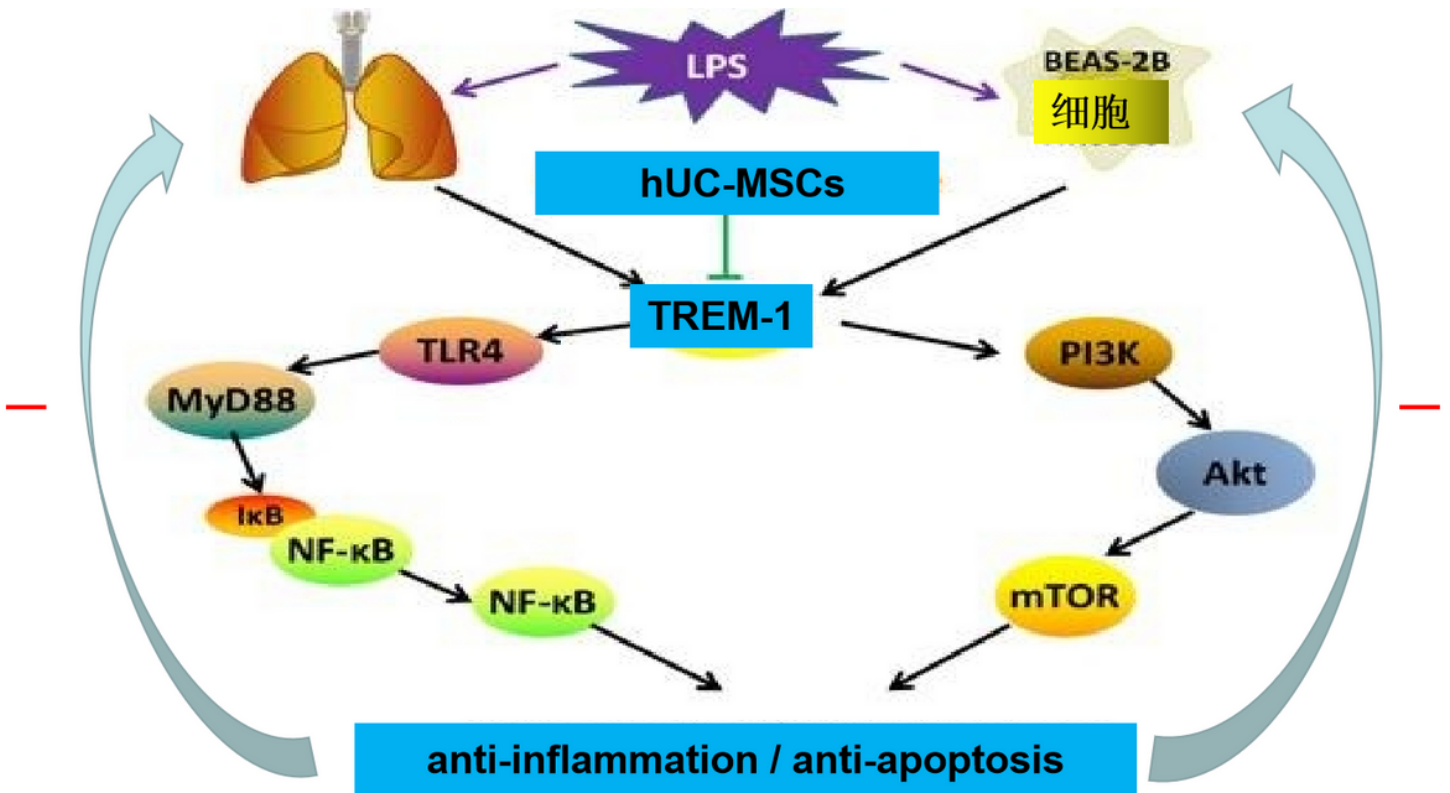


Figure 10

The role of hUC-MSCs in the therapy of ALI and their probable mechanisms of action.

hUC-MSCs can exert anti-inflammation and anti-apoptosis effect on ALI or LPS-induced BEAS-2B injury by reducing TREM-1 expression, which perhaps linked to the TLR4/MyD88 pathway and the phosphorylation of PI3K/Akt.